Supplementary Information for

# Depletion of gaseous polycyclic aromatic hydrocarbons by a forest canopy

S.-D. Choi[1], R. M. Staebler[2], H. Li[1,*], Y. Su[1,**], B. Gevao[1,***], T. Harner[2], F. Wania[1]

[1]Department of Physical and Environmental Sciences, University of Toronto Scarborough, 1265 Military Trail, Toronto, ON, Canada, M1C 1A4

[2]Science and Technology Branch, Environment Canada, 4905 Dufferin Street, Toronto, Ontario, Canada, M3H 5T4

*now at: Worsfold Water Quality Centre, Trent University, Peterborough, Ontario, Canada, K9J 7B8

**now at: Science and Technology Branch, Environment Canada, 4905 Dufferin Street, Toronto, Ontario, Canada, M3H 5T4

***now at: Department of Environmental Science, Environment and Urban Development Division, Kuwait Institute for Scientific Research, P.O. Box 24885, Safat 13109, Kuwait

*Correspondence to*: F. Wania (frank.wania@utoronto.ca).

**Content** **Page**

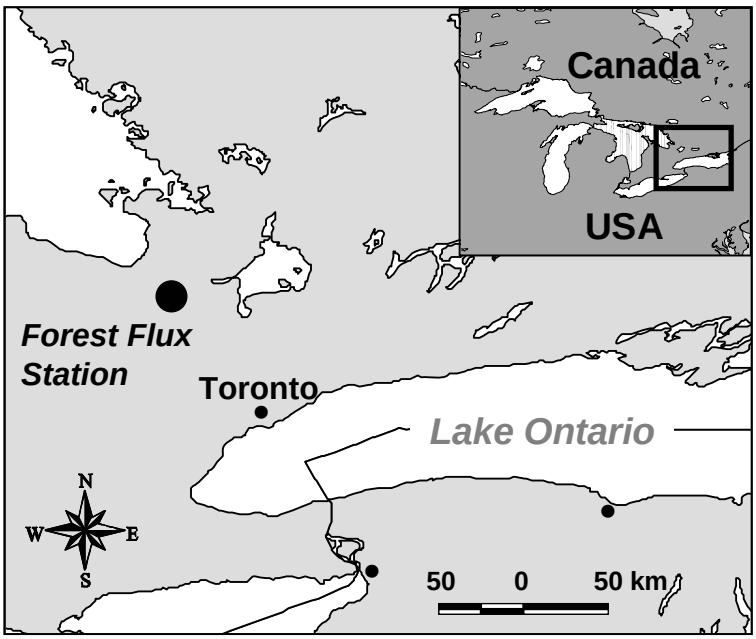


**Fig. S1** Location of the forest flux station at Borden, Ontario, Canada.

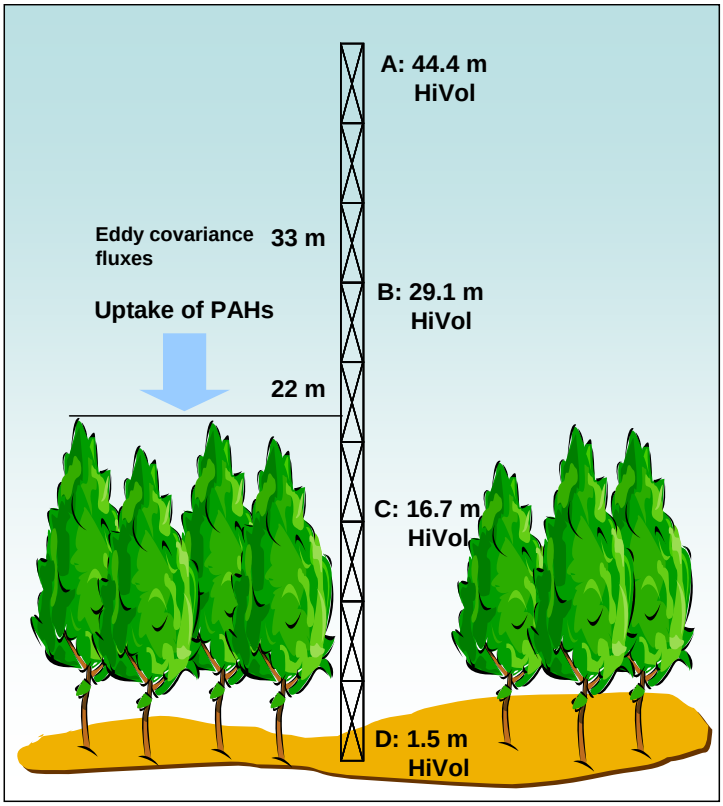


**Fig. S2** High volume air sampling at different heights (A: 44.4 m, B: 29.1 m, C: 16.7 m, and D: 1.5 m) on a 45-m scaffold tower. Eddy covariance fluxes were measured at 33 m. Average canopy height is 22 m.

**Table S1**. Air sampling time (local time) and mean temperature (°C) for 12 sampling events

| Event | Start time | End time | Average temperature |
|---|---|---|---|
| 1 | 12:49pm (April 24) | 2:54pm (April 25) | 4.6 |
| 2 | 3:04pm (April 25) | 3:00pm (April 26) | 4.8 |
| 3 | 6:23pm (May 06) | 6:11pm (May 07) | 8.2 |
| 4 | 2:32pm (May 09) | 3:02pm (May 10) | 13.0 |
| 5 | 4:48pm (May 12) | 5:08pm (May 13) | 6.0 |
| 6 | 6:25pm (May 16) | 6:25pm (May 17) | 11.6 |
| 7 | 2:40pm (May 18) | 2:48pm (May 19) | 15.9 |
| 8 | 2:10pm (May 21) | 6:52pm (May 22) | 9.0 |
| 9 | 6:52pm (May 24) | 6:19pm (May 25) | 10.2 |
| 10 | 4:34pm (May 27) | 4:59pm (May 28) | 11.7 |
| 11 | 5:38pm (May 30) | 4:56pm (May 31) | 10.7 |
| 12 | 4:49pm (June 02) | 6:16pm (June 03) | 12.0 |

**GC Temperature Program and Target Ions.** The GC oven temperature program was as follows: initial temperature held at 80°C for 1 min, increased at 10°·min$^{-1}$ to 90°C, held 1 min, 4°C·min$^{-1}$ to 130°C, 5 °C·min$^{-1}$ to 240°C, 4 °C·min$^{-1}$ to 265°C and held 16 min, then 10°C·min$^{-1}$ to 280°C and held 15 min. The interface connecting the MSD was set to temperature of 280°C, while the ion source and quadrupole temperatures were 230°C and 150°C, respectively. Ions used for SIM of target compounds were (target/qualifier): naphthalene (128/127); $d_8$-naphthalene(136/137); acenaphthylene (152/151); $d_8$-acenaphthylene(160/159); acenaphthene (153/154); fluorene (166/165); phenanthrene (178/179); $d_{10}$-phenanthrene (188/189); anthracene (178/179); fluoranthene (202/200); $d_{10}$-fluoranthene(212/213); pyrene (202/200); $d_{10}$-pyrene (212/213); benz(a)anthracene (228/226); chrysene (228/226); benzo(b)fluoranthene (252/253); benzo(k)-fluoranthene (252/253); benzo(a)pyrene (252/253); $d_{12}$-benzo(a)pyrene (264/265); indeno-(123,cd)pyrene (276/274); dibenz(a,h)anthracene (278/276); benzo(g,h,i)perylene (276/274); $d_{12}$-benzo(ghi)perylene (288/289); mirex (272/237).

**Table S2**. Average method detection limits (MDL) for 13 selected PAHs and average recoveries for 7 deuterated PAHs

| | MDL (pg·m$^{-3}$) | | | Recovery (%) | |
|---|---|---|---|---|---|
| | PUF | GFF | | PUF | GFF |
| Fluorene | 10.7 | 1.51 | $D_8$-Naphthalene | 74 | 74 |
| Phenanthrene | 27.1 | 6.51 | $D_8$-Acenaphthylene | 95 | 99 |
| Anthracene | 3.4 | 0.14 | $D_{10}$-Phenanthrene | 120 | 154 |
| Fluoranthene | 23.4 | 0.05 | $D_{10}$-Fluoranthene | 130 | 127 |
| Pyrene | 20.4 | 0.08 | $D_{10}$-Pyrene | 136 | 120 |
| Benz(a)anthracene | 0.10 | 0.10 | $D_{12}$-Benzo(a)pyrene | 93 | 108 |
| Chrysene | 0.09 | 0.09 | $D_{12}$-Benzo(ghi)perylene | 65 | 122 |
| Benzo(b)fluoranthene | 0.21 | 0.21 | | | |
| Benzo(k)fluoranthene | 0.22 | 0.22 | | | |
| Benzo(a)pyrene | 0.76 | 0.76 | | | |
| Indeno(123,cd)pyrene | 0.26 | 0.26 | | | |
| Dibenz(ah)anthracene | 0.39 | 0.39 | | | |
| Benzo(ghi)perylene | 0.23 | 0.23 | | | |

**Table S3**. Concentrations of 13 PAHs in the gas phase for 12 sampling events. BDL indicates below method detection limit

| Event | Height | ($pg \cdot m^{-3}$) | | | | | | | | | | | | |
|---|---|---|---|---|---|---|---|---|---|---|---|---|---|---|
| | | Fl | Phe | Ant | FA | PY | BaA | CR | BbF | BkF | BaP | IcdP | DahA | BghiP |
| 1 | A | 489 | 1227 | 105 | 126 | 116 | 3.6 | 5.8 | 3.0 | BDL | BDL | 2.2 | BDL | 3.8 |
| | B | 567 | 966 | 38 | 120 | 38 | 1.2 | 1.8 | 0.5 | BDL | BDL | BDL | BDL | 0.4 |
| | C | 571 | 862 | 11 | 173 | 82 | 6.5 | 11.7 | BDL | BDL | BDL | 6.6 | BDL | 5.1 |
| | D | 622 | 1481 | 178 | 131 | 191 | 9.1 | 11.5 | BDL | BDL | BDL | 5.9 | BDL | 6.2 |
| 2 | A | 525 | 1327 | 85 | 219 | 164 | 3.3 | 16.3 | 6.1 | BDL | BDL | 3.2 | BDL | 3.2 |
| | B | 572 | 1154 | 41 | 304 | 161 | 2.1 | 13.1 | 5.4 | BDL | BDL | BDL | BDL | 3.0 |
| | C | 575 | 979 | 17 | 187 | 121 | 4.3 | 14.9 | 6.8 | BDL | BDL | 4.2 | BDL | 4.8 |
| | D | 509 | 1155 | 104 | 110 | 132 | 3.6 | 9.5 | 4.8 | BDL | BDL | BDL | BDL | 3.0 |
| 3 | A | 441 | 1676 | 146 | 250 | 241 | 3.1 | 10.9 | 2.3 | 1.0 | BDL | BDL | BDL | 0.7 |
| | B | 380 | 1815 | 203 | 256 | 211 | 3.7 | 12.5 | 2.5 | BDL | BDL | BDL | BDL | 0.6 |
| | C | 395 | 1073 | 21 | 264 | 120 | 3.6 | 11.7 | 3.5 | BDL | BDL | 0.7 | BDL | 1.0 |
| | D | 341 | 1432 | 113 | 199 | 204 | 5.0 | 9.9 | 2.5 | BDL | BDL | 0.5 | BDL | 0.6 |
| 4 | A | 993 | 2444 | 216 | 315 | 337 | 5.1 | 13.9 | 7.2 | 2.6 | BDL | 1.7 | BDL | 2.2 |
| | B | 944 | 1275 | 71 | 275 | 116 | 2.7 | 12.3 | 1.9 | BDL | BDL | BDL | BDL | BDL |
| | C | 771 | 1008 | BDL | 305 | 84 | 5.1 | 13.7 | 10.5 | 3.6 | BDL | 5.0 | 0.8 | 5.4 |
| | D | 677 | 1905 | 191 | 290 | 260 | 5.0 | 11.3 | 2.9 | BDL | BDL | 0.7 | BDL | 1.7 |
| 5 | A | 237 | 763 | 83 | 114 | 143 | 2.5 | 5.9 | 1.3 | BDL | BDL | BDL | BDL | 1.2 |
| | B | 213 | 560 | 45 | 102 | 82 | 2.0 | 6.5 | 1.6 | BDL | BDL | BDL | BDL | BDL |
| | C | 170 | 348 | 12 | 87 | 50 | 2.1 | 6.3 | 3.2 | BDL | BDL | 0.4 | BDL | 0.5 |
| | D | 360 | 1430 | 164 | 140 | 249 | 3.0 | 4.9 | 1.7 | BDL | BDL | 0.5 | BDL | 0.6 |
| 6 | A | 733 | 1271 | 71 | 232 | 167 | 1.4 | 7.6 | 1.2 | BDL | BDL | 0.2 | BDL | 0.3 |
| | B | 804 | 1107 | 54 | 164 | 81 | 1.3 | 6.4 | 1.2 | BDL | BDL | BDL | BDL | BDL |
| | C | 815 | 841 | BDL | 214 | 69 | 2.5 | 8.8 | 1.9 | BDL | BDL | 0.7 | BDL | 0.8 |
| | D | 724 | 1478 | 146 | 169 | 183 | 3.4 | 6.8 | 2.1 | BDL | BDL | 0.4 | BDL | 0.6 |
| 7 | A | 700 | 2474 | 224 | 300 | 378 | 6.9 | 19.0 | 8.7 | 3.7 | 4.8 | 4.0 | 0.4 | 3.4 |
| | B | 701 | 1511 | 109 | 289 | 175 | 10.9 | 23.1 | 8.7 | 4.3 | 6.5 | 6.2 | 0.6 | 4.3 |
| | C | 818 | 877 | BDL | 212 | 78 | 4.1 | 15.3 | 8.6 | 4.8 | 7.5 | 5.6 | 0.5 | 3.7 |
| | D | 526 | 2584 | 381 | 129 | 355 | 7.3 | 9.5 | 7.9 | 3.2 | 4.9 | 4.0 | BDL | 3.6 |
| 8 | A | 351 | 991 | 66 | 113 | 142 | 2.4 | 5.2 | 2.0 | 0.9 | BDL | 1.1 | BDL | 1.0 |
| | B | 323 | 604 | 20 | 99 | 51 | 0.8 | 3.8 | BDL | BDL | BDL | BDL | BDL | BDL |
| | C | 312 | 523 | BDL | 94 | 34 | 5.5 | 10.9 | 2.8 | BDL | BDL | 1.0 | BDL | 1.3 |
| | D | 307 | 1171 | 152 | 83 | 158 | 4.5 | 5.2 | 3.5 | 2.1 | BDL | 1.1 | BDL | 1.2 |

**Table S3**. Continued

| Event | Height | ($pg \cdot m^{-3}$) | | | | | | | | | | | | |
|---|---|---|---|---|---|---|---|---|---|---|---|---|---|---|
| | | Fl | Phe | Ant | FA | PY | BaA | CR | BbF | BkF | BaP | IcdP | DahA | BghiP |
| 9 | A | 501 | 1741 | 102 | 304 | 301 | 4.3 | 19.0 | 5.0 | 1.4 | 0.8 | 1.0 | BDL | 1.0 |
| | B | 432 | 885 | 34 | 204 | 115 | 4.3 | 12.7 | 4.4 | 1.5 | BDL | BDL | BDL | BDL |
| | C | 424 | 799 | BDL | 188 | 86 | 3.7 | 12.1 | 5.6 | 1.4 | BDL | 1.8 | BDL | 2.4 |
| | D | 419 | 1138 | 57 | 106 | 133 | 2.8 | 6.4 | 2.4 | 0.7 | BDL | 0.3 | BDL | 0.4 |
| 10 | A | 250 | 1240 | 109 | 114 | 171 | 2.3 | 7.4 | 2.1 | BDL | BDL | BDL | BDL | 0.2 |
| | B | 256 | 753 | 32 | 114 | 77 | 1.7 | 6.4 | 1.8 | BDL | BDL | BDL | BDL | BDL |
| | C | 129 | 269 | 4 | 93 | 37 | 1.7 | 5.3 | 1.8 | BDL | BDL | BDL | BDL | 0.3 |
| | D | 261 | 1659 | 63 | 108 | 238 | 3.7 | 5.9 | 2.3 | 0.7 | BDL | 0.4 | BDL | 0.4 |
| 11 | A | 287 | 2489 | 38 | 437 | 408 | 19.6 | 34.3 | 14.9 | 5.7 | BDL | 1.0 | BDL | 0.9 |
| | B | 239 | 1310 | 39 | 338 | 189 | 19.1 | 26.4 | 26.1 | 7.2 | BDL | 0.8 | BDL | 0.6 |
| | C | 255 | 1255 | 15 | 293 | 143 | 17.7 | 25.1 | 27.2 | 8.2 | BDL | 2.2 | BDL | 1.8 |
| | D | 276 | 2142 | 168 | 257 | 311 | 18.7 | 21.1 | 22.4 | 7.9 | BDL | 1.7 | BDL | 1.1 |
| 12 | A | 123 | 1138 | 76 | 142 | 169 | 4.2 | 17.1 | 5.0 | BDL | BDL | BDL | BDL | 0.6 |
| | B | 91 | 724 | 37 | 103 | 71 | 4.4 | 13.8 | 0.9 | BDL | BDL | BDL | BDL | BDL |
| | C | 98 | 475 | 5 | 115 | 64 | 6.5 | 13.5 | 6.6 | BDL | BDL | 2.0 | BDL | 2.0 |
| | D | 126 | 1621 | 109 | 122 | 282 | 9.8 | 10.6 | 5.3 | 1.1 | BDL | 0.8 | BDL | 0.7 |

Fl=Fluorene, Phe=Phenanthrene, Ant=Anthracene, FA=Fluoranthene, PY=Pyrene, BaA=Benz(a)anthracene, CR=Chrysene, BbF=Benzo(b)fluoranthene, BkF=Benzo(k)fluoranthene, BaP=Benzo(a)pyrene, IcdP=Indeno(123,cd)pyrene, DahA=Dibenz(ah)anthracene, BghiP=Benzo(ghi)perylene

**Table S4**. Concentrations of 13 PAHs in the particle phase for 12 sampling events. BDL indicates below method detection limit

| Event | Height | ($pg \cdot m^{-3}$) | | | | | | | | | | | | |
|---|---|---|---|---|---|---|---|---|---|---|---|---|---|---|
| | | Fl | Phe | Ant | FA | PY | BaA | CR | BbF | BkF | BaP | IcdP | DahA | BghiP |
| 1 | A | 1.3 | 15.4 | 4.4 | 49 | 43 | 29 | 34 | 48 | 21 | 30 | 37 | 9 | 37 |
| | B | 1.8 | 23.5 | 3.6 | 72 | 53 | 37 | 61 | 80 | 33 | 30 | 60 | 12 | 54 |
| | C | 1.6 | 24.5 | 4.8 | 65 | 56 | 40 | 55 | 57 | 29 | 38 | 52 | 11 | 40 |
| | D | 1.3 | 16.5 | 4.4 | 55 | 55 | 43 | 49 | 50 | 25 | 39 | 44 | 9 | 37 |
| 2 | A | 1.3 | 11.3 | 3.6 | 31 | 29 | 24 | 39 | 54 | 23 | 28 | 43 | 10 | 37 |
| | B | 1.5 | 12.6 | 3.9 | 39 | 29 | 24 | 42 | 62 | 28 | 30 | 52 | 11 | 43 |
| | C | 1.4 | 9.8 | 3.5 | 31 | 24 | 20 | 35 | 45 | 23 | 23 | 34 | 9 | 30 |
| | D | 1.3 | 9.5 | 3.4 | 34 | 26 | 22 | 34 | 49 | 22 | 27 | 43 | 10 | 37 |
| 3 | A | 0.9 | BDL | 3.0 | 9 | 8 | 4 | 15 | 16 | 10 | 7 | 13 | 4 | 14 |
| | B | 1.0 | BDL | 3.1 | 15 | 14 | 10 | 16 | 10 | 6 | 3 | 12 | 5 | 13 |
| | C | 0.9 | BDL | 3.0 | 8 | 8 | 5 | 14 | 14 | 5 | 4 | 11 | 2 | 11 |
| | D | 0.8 | BDL | BDL | 7 | 7 | 9 | 12 | 13 | 5 | 4 | 11 | 2 | 11 |
| 4 | A | 2.0 | 11.6 | 3.9 | 23 | 23 | 16 | 31 | 53 | 21 | 22 | 32 | 10 | 36 |
| | B | 2.2 | 11.0 | 4.1 | 29 | 25 | 19 | 40 | 66 | 26 | 28 | 42 | 11 | 44 |
| | C | 2.0 | 8.1 | 3.9 | 20 | 19 | 17 | 32 | 46 | 19 | 21 | 28 | 9 | 31 |
| | D | 1.9 | 8.3 | 3.8 | 23 | 23 | 20 | 35 | 57 | 21 | 28 | 42 | 11 | 45 |
| 5 | A | 1.4 | BDL | BDL | 6 | 6 | 4 | 5 | 3 | 2 | 3 | 6 | 2 | 7 |
| | B | BDL | BDL | BDL | 4 | 4 | 5 | 5 | 7 | 5 | 3 | 7 | 5 | 7 |
| | C | 1.5 | BDL | BDL | 7 | 7 | 4 | 6 | 9 | 2 | 3 | 6 | BDL | 7 |
| | D | 1.3 | BDL | BDL | 6 | 6 | 3 | 5 | 7 | BDL | 3 | 6 | BDL | 7 |
| 6 | A | 1.8 | 6.6 | 3.5 | 17 | 16 | 11 | 16 | 20 | 11 | 7 | 18 | 7 | 18 |
| | B | 1.9 | 6.5 | 3.6 | 17 | 16 | 10 | 15 | 16 | 8 | 5 | 13 | 5 | 14 |
| | C | 1.7 | 8.4 | 3.6 | 15 | 11 | 9 | 13 | 14 | 6 | 2 | 14 | 5 | 13 |
| | D | 3.8 | 7.3 | BDL | 10 | 14 | 6 | 9 | 11 | 7 | 4 | 10 | 5 | 11 |
| 7 | A | 3.6 | 14.2 | BDL | 32 | 28 | 17 | 31 | 47 | 24 | 27 | 39 | 9 | 42 |
| | B | 3.6 | 12.9 | BDL | 28 | 25 | 19 | 34 | 49 | 23 | 25 | 48 | 10 | 46 |
| | C | 1.3 | 8.9 | 4.3 | 31 | 28 | 24 | 40 | 60 | 28 | 30 | 55 | 11 | 52 |
| | D | 3.3 | 8.4 | BDL | 18 | 21 | 13 | 20 | 47 | 21 | 29 | 44 | 9 | 35 |
| 8 | A | 0.8 | 3.3 | BDL | 14 | 14 | 12 | 15 | 25 | 9 | 7 | 18 | 5 | 18 |
| | B | 0.9 | 4.5 | BDL | 15 | 20 | 11 | 17 | 30 | 12 | 14 | 23 | 6 | 23 |
| | C | 0.8 | 6.5 | BDL | 11 | 15 | 9 | 16 | 23 | 10 | 9 | 18 | 5 | 17 |
| | D | 0.7 | 2.1 | BDL | 8 | 7 | 9 | 11 | 16 | 11 | 8 | 12 | 4 | 13 |

**Table S4**. Continued

| Event | Height | (pg·m$^{-3}$) | | | | | | | | | | | | |
|---|---|---|---|---|---|---|---|---|---|---|---|---|---|---|
| | | Fl | Phe | Ant | FA | PY | BaA | CR | BbF | BkF | BaP | IcdP | DahA | BghiP |
| 9 | A | 0.9 | BDL | BDL | 14 | 14 | 7 | 10 | 18 | 10 | 7 | 18 | 6 | 16 |
| | B | 0.9 | 3.0 | BDL | 11 | 10 | 12 | 16 | 24 | 15 | 12 | 22 | 6 | 20 |
| | C | 0.8 | 4.6 | BDL | 5 | 11 | 5 | 6 | 10 | 6 | 4 | 8 | 5 | 8 |
| | D | 0.7 | 4.9 | BDL | 7 | 7 | 6 | 6 | 14 | 8 | 6 | 17 | 5 | 14 |
| 10 | A | 0.4 | 3.5 | 2.1 | 18 | 15 | 6 | 15 | 21 | 10 | 13 | 19 | 6 | 17 |
| | B | 0.4 | 3.4 | 1.5 | 22 | 16 | 7 | 11 | 17 | 10 | 7 | 15 | 6 | 13 |
| | C | 0.4 | 2.7 | 0.6 | 15 | 13 | 7 | 11 | 12 | 8 | 5 | 12 | 5 | 10 |
| | D | 0.4 | BDL | BDL | 12 | 10 | 8 | 12 | 17 | 10 | 8 | 18 | 5 | 15 |
| 11 | A | 0.3 | BDL | BDL | 8 | 10 | 5 | 5 | 13 | 8 | 4 | 22 | 6 | 17 |
| | B | 0.3 | BDL | 1.4 | 9 | 6 | 8 | 11 | 26 | 11 | 5 | 43 | 9 | 35 |
| | C | 3.0 | 3.7 | BDL | 5 | 6 | 6 | 7 | 18 | 11 | 6 | 36 | 8 | 28 |
| | D | 0.2 | 3.9 | BDL | 6 | 7 | 6 | 7 | 20 | 12 | 7 | 45 | 10 | 36 |
| 12 | A | 0.2 | BDL | 1.4 | 11 | 11 | 15 | 24 | 48 | 23 | 20 | 33 | 10 | 26 |
| | B | 0.3 | BDL | 1.6 | 14 | 15 | 17 | 26 | 45 | 21 | 21 | 39 | 11 | 28 |
| | C | 0.3 | BDL | BDL | 12 | 12 | 13 | 20 | 36 | 17 | 16 | 25 | 11 | 20 |
| | D | 0.3 | BDL | BDL | 10 | 11 | 9 | 13 | 25 | 11 | 8 | 24 | 7 | 20 |

Fl=Fluorene, Phe=Phenanthrene, Ant=Anthracene, FA=Fluoranthene, PY=Pyrene, BaA=Benz(a)anthracene, CR=Chrysene, BbF=Benzo(b)fluoranthene, BkF=Benzo(k)fluoranthene, BaP=Benzo(a)pyrene, IcdP=Indeno(123,cd)pyrene, DahA=Dibenz(ah)anthracene, BghiP=Benzo(ghi)perylene

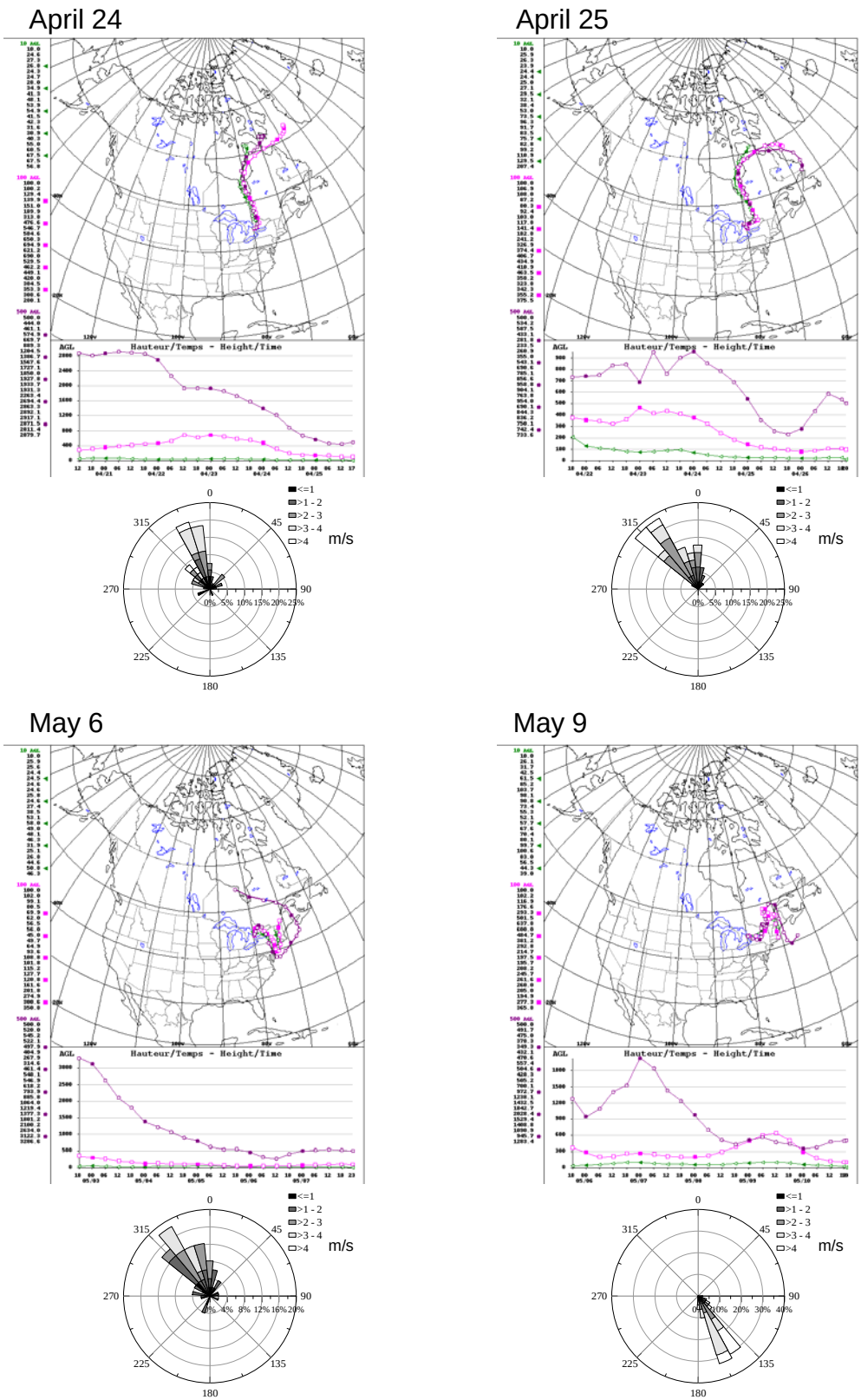


**Fig. S3** Five-day back trajectories at three heights (10, 100, 500 m) and wind-rose diagrams during sampling events.

May 12

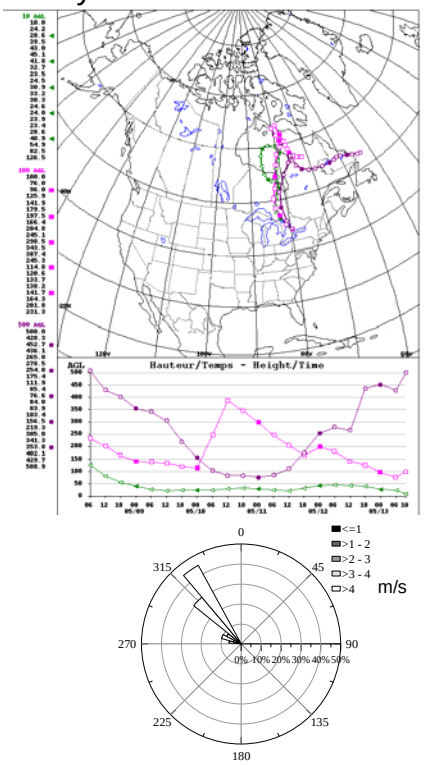


May 16

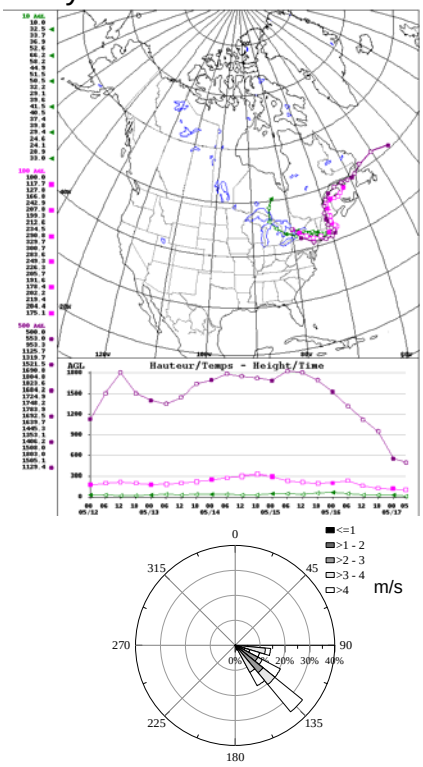


May 18

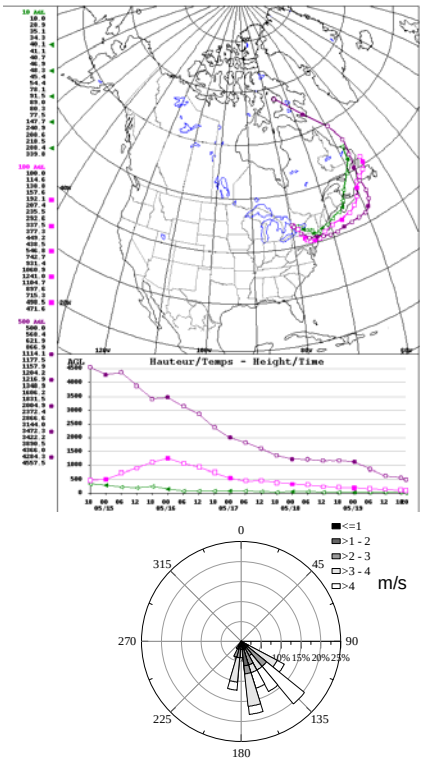


May 21

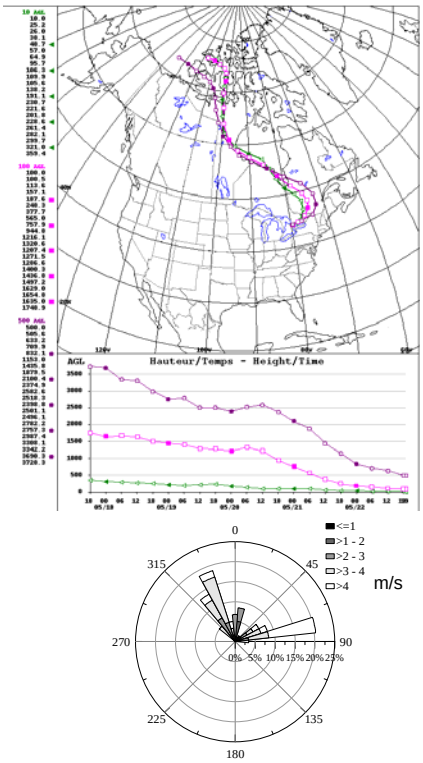


**Fig. S3** Continued.

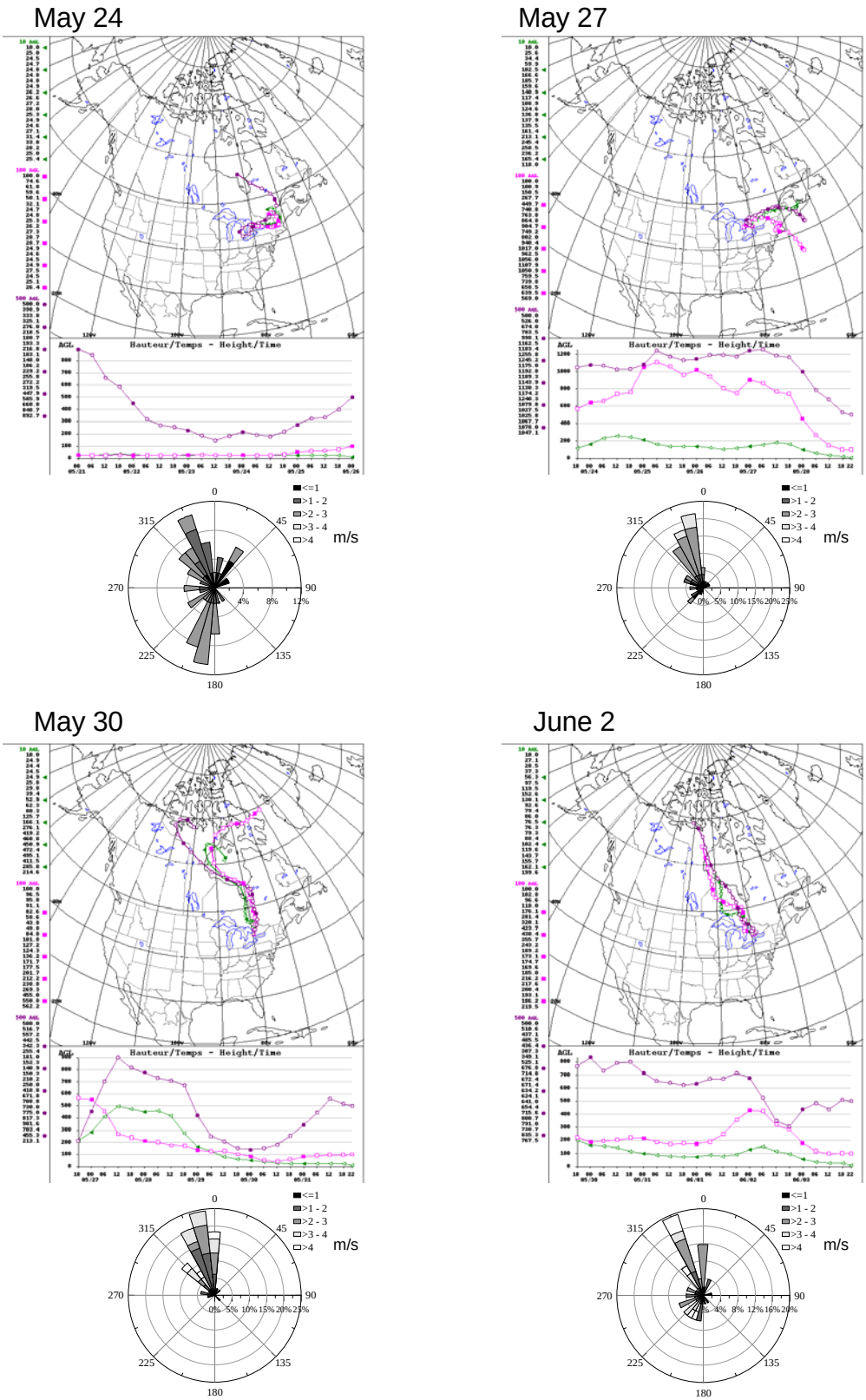


**Fig. S3** Continued.

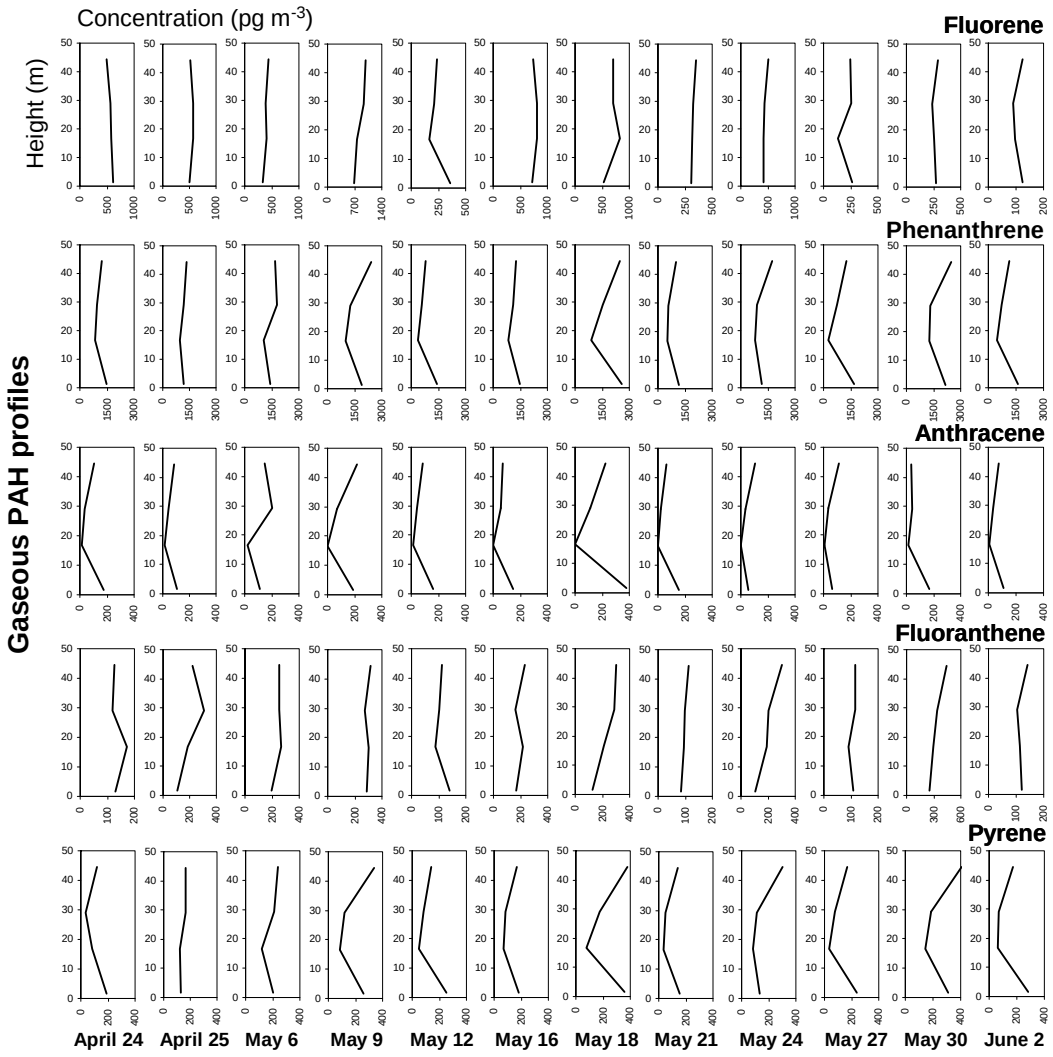


**Fig. S4** Vertical profiles of gaseous and particulate PAHs measured at the 4 different heights.

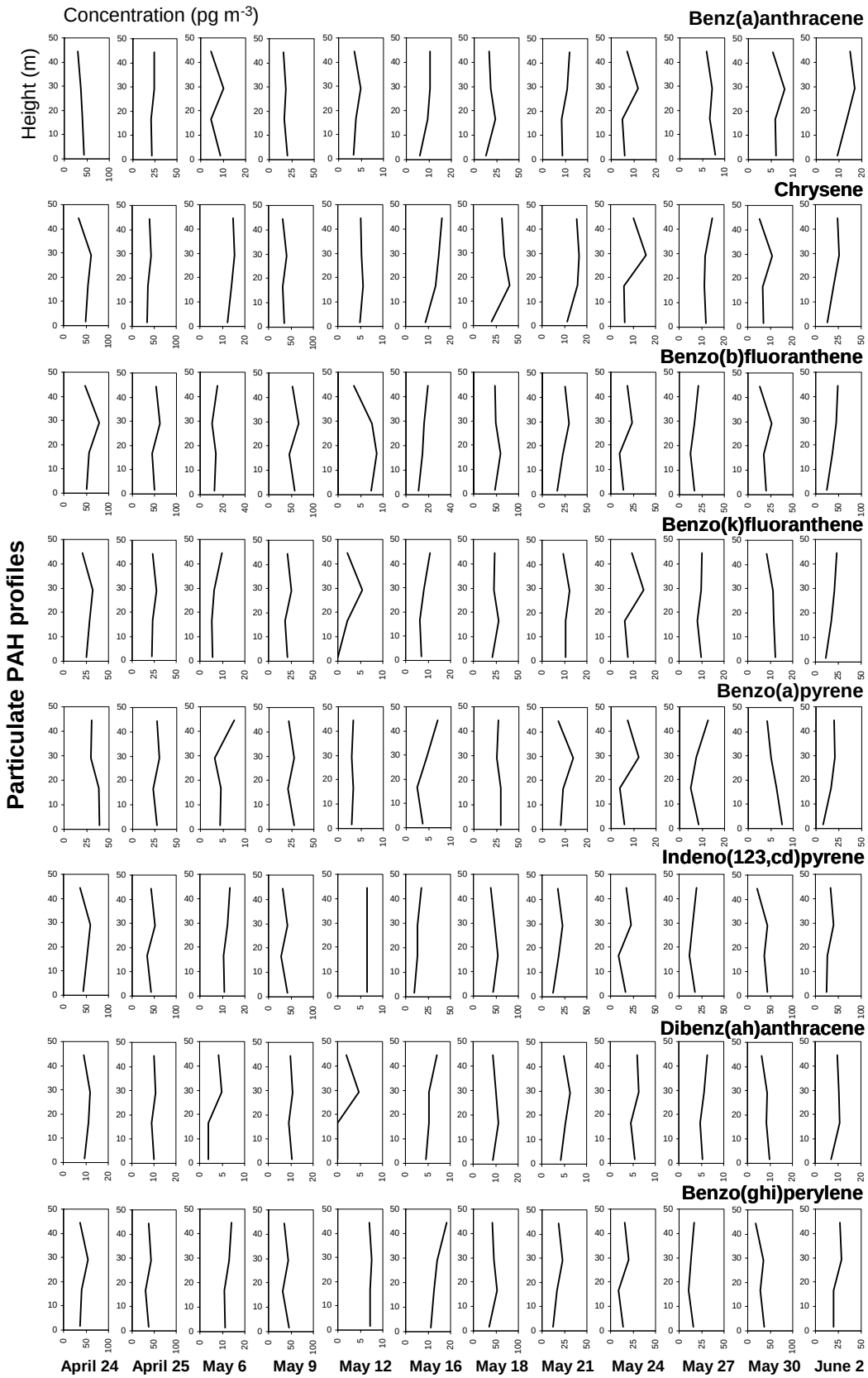


**Fig. S4** Continued.

**Table S5**. Measured particle-bound percentages of 13 PAHs for 12 sampling events

| Event | Height | (%) | | | | | | | | | | | | |
|---|---|---|---|---|---|---|---|---|---|---|---|---|---|---|
| | | Fl | Phe | Ant | FA | PY | BaA | CR | BbF | BkF | BaP | IcdP | DahA | BghiP |
| 1 | A | 0.3 | 1.2 | 4 | 28 | 27 | 89 | 85 | 94 | 100 | 100 | 95 | 100 | 91 |
| | B | 0.3 | 2.4 | 9 | 37 | 58 | 97 | 97 | 99 | 100 | 100 | 100 | 100 | 99 |
| | C | 0.3 | 2.8 | 31 | 27 | 41 | 86 | 82 | 100 | 100 | 100 | 89 | 100 | 89 |
| | D | 0.2 | 1.1 | 2 | 30 | 22 | 83 | 81 | 100 | 100 | 100 | 88 | 100 | 86 |
| 2 | A | 0.3 | 0.8 | 4 | 13 | 15 | 88 | 70 | 90 | 100 | 100 | 93 | 100 | 92 |
| | B | 0.3 | 1.1 | 9 | 11 | 15 | 92 | 76 | 92 | 100 | 100 | 100 | 100 | 94 |
| | C | 0.2 | 1.0 | 17 | 14 | 17 | 83 | 70 | 87 | 100 | 100 | 89 | 100 | 86 |
| | D | 0.2 | 0.8 | 3 | 23 | 16 | 86 | 78 | 91 | 100 | 100 | 100 | 100 | 93 |
| 3 | A | 0.2 | 0.0 | 2 | 3 | 3 | 59 | 57 | 87 | 91 | 100 | 100 | 100 | 96 |
| | B | 0.3 | 0.0 | 2 | 6 | 6 | 73 | 55 | 81 | 100 | 100 | 100 | 100 | 96 |
| | C | 0.2 | 0.0 | 13 | 3 | 6 | 56 | 55 | 80 | 100 | 100 | 93 | 100 | 92 |
| | D | 0.2 | 0.0 | 0 | 4 | 3 | 64 | 56 | 84 | 100 | 100 | 96 | 100 | 95 |
| 4 | A | 0.2 | 0.5 | 2 | 7 | 6 | 76 | 69 | 88 | 89 | 100 | 95 | 100 | 94 |
| | B | 0.2 | 0.9 | 6 | 10 | 18 | 87 | 77 | 97 | 100 | 100 | 100 | 100 | 100 |
| | C | 0.3 | 0.8 | 100 | 6 | 19 | 77 | 70 | 82 | 84 | 100 | 85 | 92 | 85 |
| | D | 0.3 | 0.4 | 2 | 7 | 8 | 80 | 76 | 95 | 100 | 100 | 98 | 100 | 96 |
| 5 | A | 0.6 | 0.0 | 0 | 5 | 4 | 59 | 46 | 72 | 100 | 100 | 100 | 100 | 85 |
| | B | 0.0 | 0.0 | 0 | 4 | 5 | 72 | 45 | 82 | 100 | 100 | 100 | 100 | 100 |
| | C | 0.8 | 0.0 | 0 | 7 | 12 | 64 | 47 | 73 | 100 | 100 | 94 | 0 | 94 |
| | D | 0.4 | 0.0 | 0 | 4 | 2 | 53 | 50 | 81 | 0 | 100 | 93 | 0 | 92 |
| 6 | A | 0.2 | 0.5 | 5 | 7 | 9 | 88 | 68 | 94 | 100 | 100 | 99 | 100 | 98 |
| | B | 0.2 | 0.6 | 6 | 9 | 16 | 89 | 69 | 93 | 100 | 100 | 100 | 100 | 100 |
| | C | 0.2 | 1.0 | 100 | 6 | 13 | 79 | 61 | 89 | 100 | 100 | 95 | 100 | 94 |
| | D | 0.5 | 0.5 | 0 | 6 | 7 | 63 | 56 | 84 | 100 | 100 | 96 | 100 | 95 |
| 7 | A | 0.5 | 0.6 | 0 | 10 | 7 | 71 | 62 | 84 | 86 | 85 | 91 | 96 | 93 |
| | B | 0.5 | 0.8 | 0 | 9 | 13 | 63 | 60 | 85 | 84 | 79 | 88 | 94 | 91 |
| | C | 0.2 | 1.0 | 100 | 13 | 26 | 85 | 72 | 88 | 85 | 80 | 91 | 96 | 93 |
| | D | 0.6 | 0.3 | 0 | 12 | 5 | 64 | 68 | 86 | 87 | 86 | 92 | 100 | 91 |
| 8 | A | 0.2 | 0.3 | 0 | 11 | 9 | 83 | 75 | 93 | 92 | 100 | 94 | 100 | 95 |
| | B | 0.3 | 0.7 | 0 | 13 | 28 | 93 | 82 | 100 | 100 | 100 | 100 | 100 | 100 |
| | C | 0.3 | 1.2 | 0 | 11 | 31 | 61 | 59 | 89 | 100 | 100 | 95 | 100 | 93 |
| | D | 0.2 | 0.2 | 0 | 8 | 4 | 66 | 68 | 83 | 84 | 100 | 92 | 100 | 91 |

**Table S5**. Continued

| Event | Height | (%) | | | | | | | | | | | | |
|---|---|---|---|---|---|---|---|---|---|---|---|---|---|---|
| | | Fl | Phe | Ant | FA | PY | BaA | CR | BbF | BkF | BaP | IcdP | DahA | BghiP |
| 9 | A | 0.2 | 0.0 | 0 | 4 | 5 | 62 | 35 | 79 | 88 | 90 | 95 | 100 | 94 |
| | B | 0.2 | 0.3 | 0 | 5 | 8 | 74 | 55 | 84 | 91 | 100 | 100 | 100 | 100 |
| | C | 0.2 | 0.6 | 0 | 3 | 11 | 57 | 33 | 63 | 82 | 100 | 82 | 100 | 77 |
| | D | 0.2 | 0.4 | 0 | 6 | 5 | 68 | 50 | 85 | 92 | 100 | 98 | 100 | 97 |
| 10 | A | 0.2 | 0.3 | 2 | 14 | 8 | 72 | 67 | 91 | 100 | 100 | 100 | 100 | 99 |
| | B | 0.2 | 0.4 | 4 | 16 | 17 | 81 | 64 | 90 | 100 | 100 | 100 | 100 | 100 |
| | C | 0.3 | 1.0 | 14 | 14 | 26 | 80 | 68 | 87 | 100 | 100 | 100 | 100 | 97 |
| | D | 0.1 | 0.0 | 0 | 10 | 4 | 68 | 67 | 88 | 94 | 100 | 98 | 100 | 98 |
| 11 | A | 0.1 | 0.0 | 0 | 2 | 2 | 21 | 13 | 47 | 59 | 100 | 96 | 100 | 95 |
| | B | 0.1 | 0.0 | 3 | 3 | 3 | 30 | 29 | 50 | 61 | 100 | 98 | 100 | 98 |
| | C | 1.2 | 0.3 | 0 | 2 | 4 | 25 | 21 | 39 | 58 | 100 | 94 | 100 | 94 |
| | D | 0.1 | 0.2 | 0 | 2 | 2 | 25 | 25 | 47 | 61 | 100 | 96 | 100 | 97 |
| 12 | A | 0.2 | 0.0 | 2 | 7 | 6 | 78 | 58 | 91 | 100 | 100 | 100 | 100 | 98 |
| | B | 0.4 | 0.0 | 4 | 12 | 18 | 79 | 65 | 98 | 100 | 100 | 100 | 100 | 100 |
| | C | 0.3 | 0.0 | 0 | 9 | 16 | 68 | 60 | 84 | 100 | 100 | 93 | 100 | 91 |
| | D | 0.2 | 0.0 | 0 | 7 | 4 | 48 | 55 | 82 | 91 | 100 | 97 | 100 | 97 |

Fl=Fluorene, Phe=Phenanthrene, Ant=Anthracene, FA=Fluoranthene, PY=Pyrene, BaA=Benz(a)anthracene, CR=Chrysene, BbF=Benzo(b)fluoranthene, BkF=Benzo(k)fluoranthene, BaP=Benzo(a)pyrene, IcdP=Indeno(123,cd)pyrene, DahA=Dibenz(ah)anthracene, BghiP=Benzo(ghi)perylene

**Gas/Particle Partitioning.** Because Fig. 2 indicated that rapid uptake of gaseous PAHs by the forest canopy is expected to affect the gas/particle (G/P) partitioning behavior, this was further explored by relating the fraction in the particle phase (Table S5) to a PAH's vapor pressure. Adopting the approach by Su et al. (2006), the fraction in the particle phase ($\Phi$) was calculated from the PAH data (Table S5) and was fitted using the following two equations:

One-parameter model: $$\Phi = A / (P_L + A) \quad (1)$$

Two-parameter model: $$\Phi = 1 / (1 + 10^{-m \cdot \log(P_L/\mathrm{Pa}) - b'}) \quad (2)$$

where $P_L$ is the vapor pressure of the sub-cooled liquid (Pa), taken from Lei et al. (2002), and $A$, $m$, and $b'$ are fitting parameters. Regression results of all 48 samples are listed in Table S6, and plots of observed G/P partitioning and fitting curves for the two models are presented in Fig. S5. Both models have average-correlation coefficients of 0.96 and 0.97, respectively, and their fitting curves for the same sample are very similar. The curves for level B (29.1 m) are generally shifted to the right, implying an increased contribution of particulate PAHs above the forest canopy.

In order to compare G/P partitioning at different heights, fitting parameters (log $A$, $m$, and $b'$) at two heights (A-B, A-C, A-D, B-C, B-D, and C-D) were correlated (Fig. S6). Eight data sets (out of 48, 1C, 7A, 7B, 8C, 9A, 9C, 11B, and 11C in Table S6) with extreme slopes ($m > -0.6$ and $m < -2$) were excluded (Su et al., 2006). Data points clustered close to the diagonal 1:1 lines in Fig. S6, imply a small difference in the fitting parameters between two heights. According to paired students' t-test with a two-tailed distribution, significant differences ($p < 0.01$) were observed in log $A$ (A-B, B-D), $m$ (A-C), and $b'$ (A-C). This suggests that the G/P partitioning behavior above and within the canopy is indeed statistically different. As parameter $A$ is directly related to the capacity of the particles (Pankow, 1987), the red triangles for A-B to the upper right of the diagonal line (Fig. S6a) indicate that air samples at level B have a higher fraction of intermediate PAHs on particles. This is consistent with the observation of increased $\Phi$ with decreased PAH concentrations above and within the canopy (Fig. 2). Explanations for $m$ and $b'$ (Fig. S6b and c) are also possible; the higher values of $m$ and $b'$ at level C produced shallower and rightward-shifted fitting curves, resulting in higher $\Phi$ for intermediate PAHs. This supports our assertion that canopy uptake of gaseous PAHs resulted in a change in G/P partitioning.

Pankow, J. F.: Review and comparative analysis of the theories on partitioning between the gas and aerosol particulate phases in the atmosphere, Atmos. Environ., 21, 2275-2283, 1987.

**Table S6**. Regression parameters for the two different nonlinear models

| Event | Height | Two-parameter model | | | One-parameter model | |
|---|---|---|---|---|---|---|
| | | $m$ | $b'$ | $R^2$ | $A\times10^5$ | $R^2$ |
| 1 | A (44.4 m) | -0.91±0.09 | -3.37±0.33 | 0.99 | 20.2±3.0 | 0.99 |
| | B (29.1 m) | -1.10±0.19 | -3.65±0.62 | 0.99 | 49.4±5.7 | 0.99 |
| | C (16.7 m) | -0.59±0.11 | -2.14±0.39 | 0.95 | 27.2±8.4 | 0.93 |
| | D (1.5 m) | -0.82±0.11 | -3.13±0.41 | 0.98 | 16.3±3.7 | 0.97 |
| 2 | A (44.4 m) | -0.93±0.15 | -3.71±0.60 | 0.97 | 10.2±2.9 | 0.97 |
| | B (29.1 m) | -1.13±0.16 | -4.42±0.63 | 0.98 | 11.7±2.9 | 0.98 |
| | C (16.7 m) | -0.75±0.14 | -3.03±0.58 | 0.95 | 9.4±3.3 | 0.94 |
| | D (1.5 m) | -0.90±0.10 | -3.50±0.39 | 0.98 | 13.1±2.6 | 0.98 |
| 3 | A (44.4 m) | -0.75±0.10 | -3.30±0.45 | 0.98 | 4.3±0.8 | 0.98 |
| | B (29.1 m) | -0.75±0.15 | -3.15±0.66 | 0.96 | 6.4±1.9 | 0.96 |
| | C (16.7 m) | -0.70±0.12 | -3.07±0.53 | 0.97 | 4.2±1.0 | 0.96 |
| | D (1.5 m) | -0.80±0.14 | -3.40±0.61 | 0.97 | 5.4±1.2 | 0.97 |
| 4 | A (44.4 m) | -0.93±0.15 | -3.52±0.60 | 0.98 | 15.9±3.7 | 0.98 |
| | B (29.1 m) | -1.04±0.11 | -3.66±0.39 | 0.99 | 29.5±5.3 | 0.99 |
| | C (16.7 m) | -0.69±0.16 | -2.59±0.61 | 0.93 | 20.6±7.9 | 0.92 |
| | D (1.5 m) | -1.12±0.12 | -4.11±0.46 | 0.99 | 21.7±3.5 | 0.99 |
| 5 | A (44.4 m) | -0.65±0.13 | -3.00±0.63 | 0.95 | 2.5±0.8 | 0.93 |
| | B (29.1 m) | -0.69±0.16 | -3.09±0.71 | 0.95 | 3.6±1.2 | 0.94 |
| | C (16.7 m) | -0.61±0.12 | -2.72±0.55 | 0.95 | 3.4±1.2 | 0.92 |
| | D (1.5 m) | -0.66±0.11 | -3.07±0.52 | 0.97 | 2.7±0.7 | 0.96 |
| 6 | A (44.4 m) | -1.09±0.18 | -4.04±0.70 | 0.97 | 19.8±5.3 | 0.97 |
| | B (29.1 m) | -0.99±0.15 | -3.61±0.57 | 0.97 | 22.7±5.9 | 0.97 |
| | C (16.7 m) | -0.82±0.15 | -3.17±0.62 | 0.96 | 14.5±4.1 | 0.96 |
| | D (1.5 m) | -0.75±0.12 | -3.08±0.49 | 0.98 | 8.3±1.8 | 0.97 |
| 7 | A (44.4 m) | -0.60±0.09 | -2.28±0.38 | 0.96 | 18.7±5.6 | 0.95 |
| | B (29.1 m) | -0.50±0.06 | -1.99±0.26 | 0.97 | 14.1±4.5 | 0.93 |
| | C (16.7 m) | -0.63±0.13 | -2.18±0.47 | 0.93 | 42.9±16.2 | 0.92 |
| | D (1.5 m) | -0.65±0.09 | -2.53±0.37 | 0.97 | 15.0±3.6 | 0.97 |
| 8 | A (44.4 m) | -1.04±0.13 | -4.02±0.54 | 0.98 | 13.9±2.9 | 0.98 |
| | B (29.1 m) | -1.13±0.13 | -4.01±0.44 | 0.99 | 26.7±4.6 | 0.99 |
| | C (16.7 m) | -0.59±0.07 | -2.43±0.32 | 0.98 | 6.7±2.0 | 0.95 |
| | D (1.5 m) | -0.75±0.13 | -3.12±0.55 | 0.97 | 7.2±1.8 | 0.97 |

**Table S6**. Continued

| Event | | Two-parameter model | | | One-parameter model | |
|---|---|---|---|---|---|---|
| | | $m$ | $b'$ | $R^2$ | $A\times10^5$ | $R^2$ |
| 9 | A (44.4 m) | -0.57±0.10 | -2.59±0.45 | 0.95 | 3.2±1.1 | 0.92 |
| | B (29.1 m) | -0.73±0.14 | -3.01±0.59 | 0.96 | 8.2±2.4 | 0.96 |
| | C (16.7 m) | -0.46±0.10 | -2.19±0.48 | 0.90 | 2.7±1.3 | 0.83 |
| | D (1.5 m) | -0.70±0.12 | -2.93±0.53 | 0.97 | 6.6±1.8 | 0.96 |
| 10 | A (44.4 m) | -0.83±0.09 | -3.20±0.38 | 0.99 | 13.1±2.4 | 0.99 |
| | B (29.1 m) | -0.75±0.11 | -2.80±0.40 | 0.98 | 19.0±5.1 | 0.97 |
| | C (16.7 m) | -0.67±0.09 | -2.43±0.35 | 0.97 | 25.7±7.6 | 0.96 |
| | D (1.5 m) | -0.87±0.11 | -3.39±0.45 | 0.99 | 12.2±2.1 | 0.98 |
| 11 | A (44.4 m) | -0.74±0.16 | -4.06±0.94 | 0.94 | 0.3±0.1 | 0.93 |
| | B (29.1 m) | -0.58±0.11 | -2.99±0.60 | 0.94 | 0.3±0.1 | 0.90 |
| | C (16.7 m) | -0.60±0.14 | -3.22±0.78 | 0.91 | 0.3±0.1 | 0.90 |
| | D (1.5 m) | -0.61±0.12 | -3.21±0.66 | 0.94 | 0.3±0.1 | 0.92 |
| 12 | A (44.4 m) | -0.85±0.16 | -3.30±0.65 | 0.97 | 13.3±3.5 | 0.97 |
| | B (29.1 m) | -0.80±0.10 | -2.97±0.39 | 0.98 | 18.3±4.2 | 0.98 |
| | C (16.7 m) | -0.69±0.10 | -2.76±0.42 | 0.97 | 10.1±2.6 | 0.96 |
| | D (1.5 m) | -0.70±0.07 | -3.03±0.30 | 0.99 | 4.7±0.8 | 0.98 |

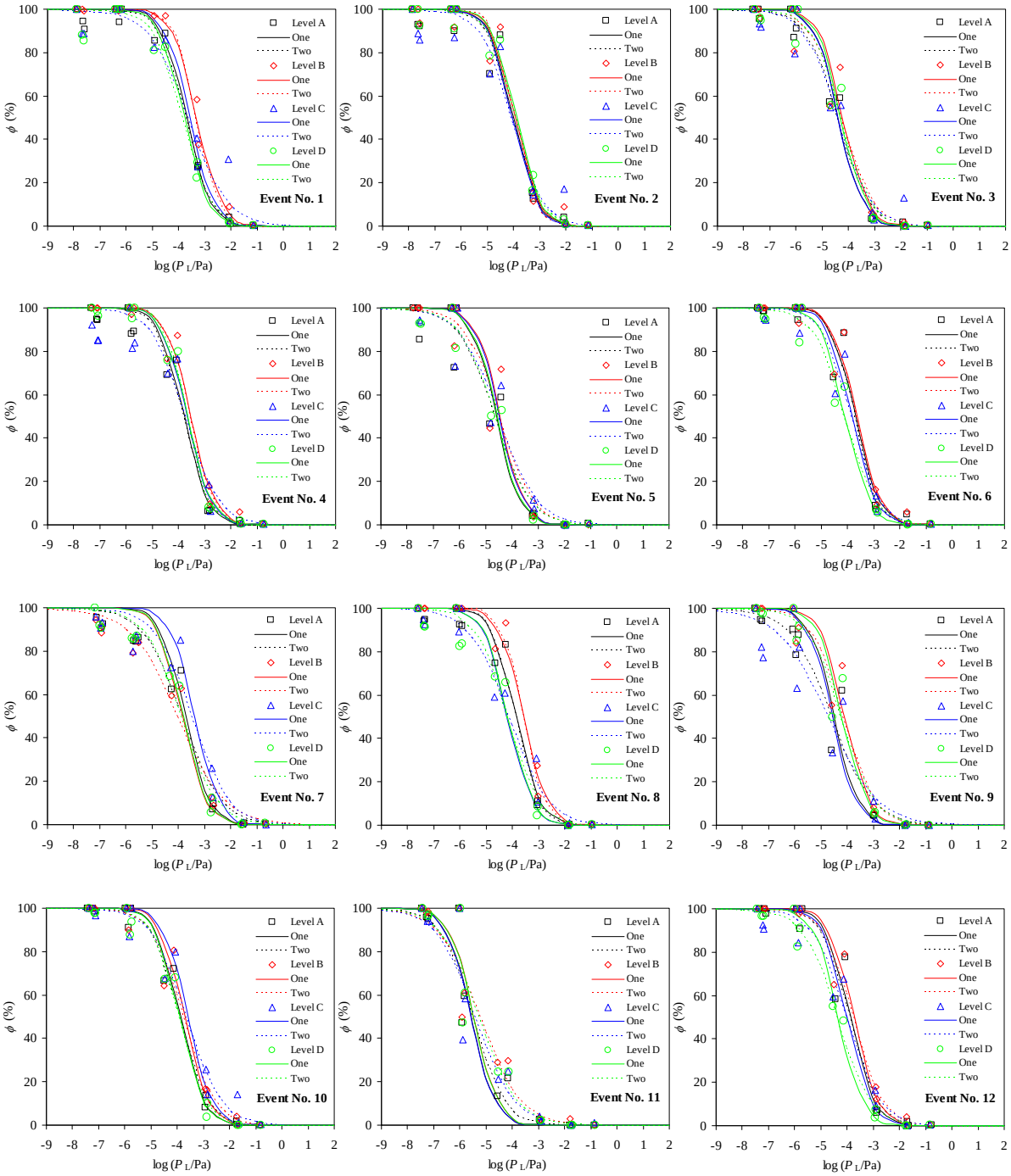


**Fig. S5** Observed gas/particle partitioning behavior of 13 PAHs for all 12 sampling events and fitting curves for the nonlinear one-parameter model and nonlinear two-parameter model.

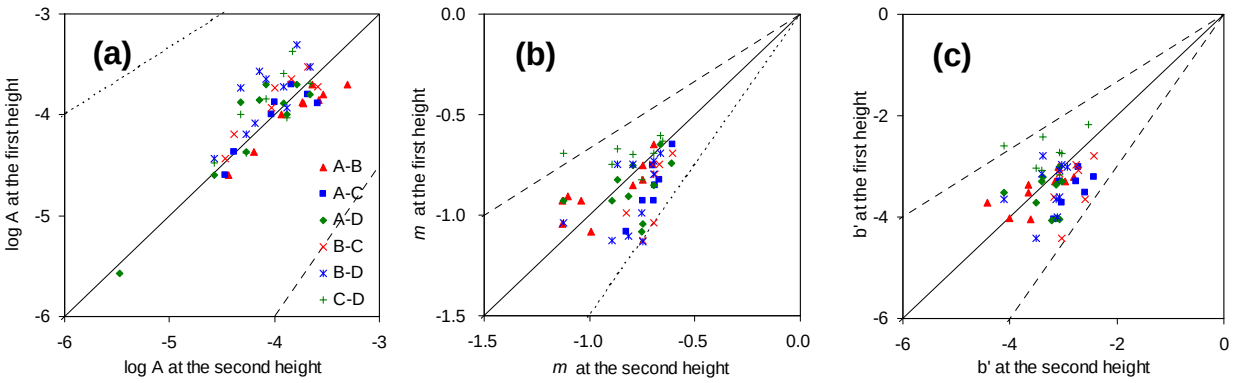


**Fig. S6** Correlation plots of the fitting parameters of log *A* (A), *m* (B), and *b'* (C) describing the gas/particle partitioning behavior of PAHs between the different heights (A-B, A-C, A-D, B-C, B-D, and C-D). The dotted lines correspond to differences between the two heights of a factor of 1.5.

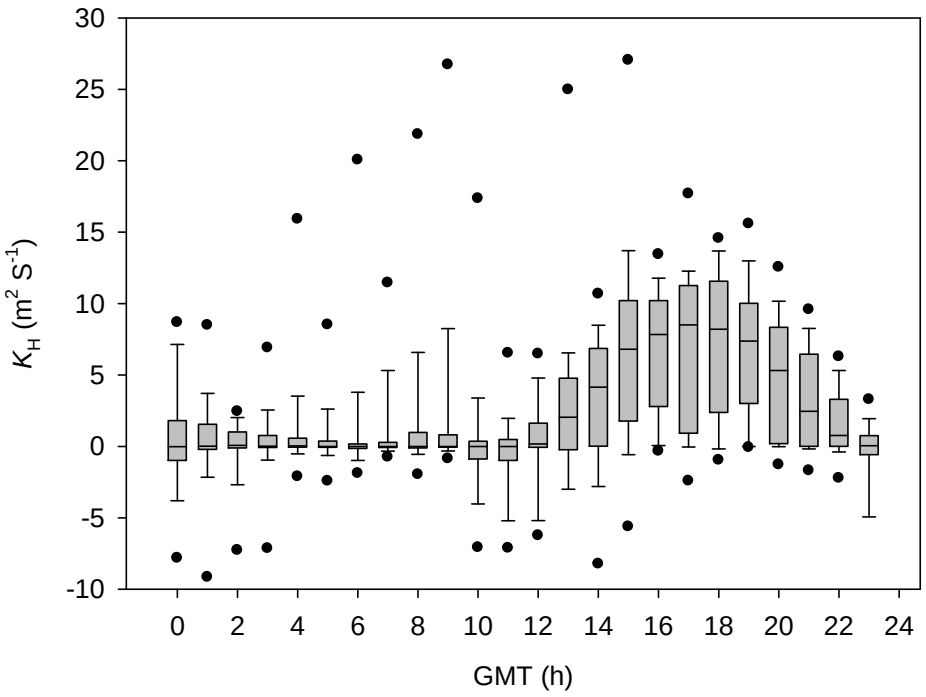


**Fig. S7** Diurnal cycle of the sensible heat diffusivity ($K_{Heat}$) measured at Borden during the period April 20–June 10, 2003. Boxes delineate the upper and lower quartile, and the line inside the box denotes the median. Whiskers span the 10$^{th}$ to 90$^{th}$ percentile range, and circles are for 5$^{th}$ and 95$^{th}$ percentiles.

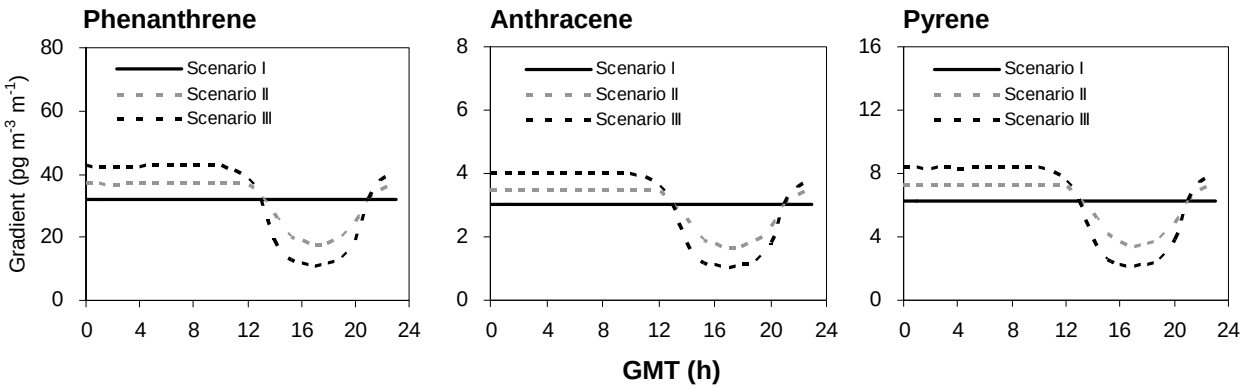


**Fig. S8** Diurnal cycle of the gradient of phenanthrene, anthracene, and pyrene for three scenarios: (I) Constant gradient throughout the 24-hour sample, (II) Gradient decreasing by 50% during the day when mixing increases, while keeping the average gradient, (III) Gradient decreasing to 25%.

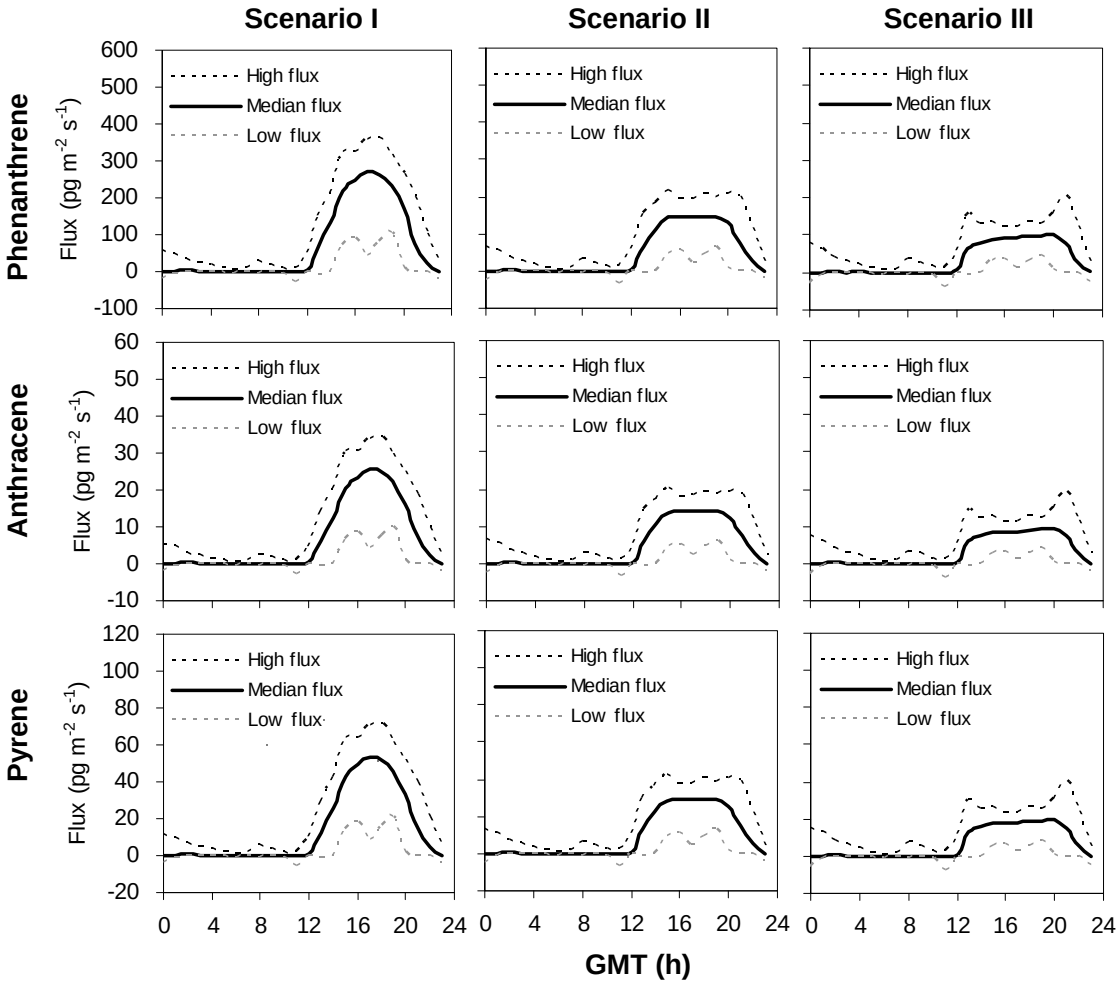


**Fig. S9** Diurnal cycles of the PAH flux to the forest canopy for three different assumptions concerning the concentration gradient d*C*/dz: (I) Constant d*C*/dz throughout 24 hours, (II) d*C*/dz decreases by 50% during the day when mixing increases, and (III) d*C*/dz decreases to 25% during the day when mixing increases. High and low fluxes were calculated using upper and lower quartiles of $K_{\mathrm{Heat.}}$

**Table S7**. Propagation of uncertainties in the input parameters to the estimates of the PAH fluxes and dry deposition velocities, based on the observed input parameter ranges. The values in gray cells exceeding the physical limit to deposition derived from the reciprocal aerodynamic resistance are considered to be unrealistic.

(a) Phenanthrene flux ($pg \cdot m^{-2} s^{-1}$)

**Scenario I:** d*C*/d*z*(day) = d*C*/d*z*(night)

| Range of d*C*/d*z* \ Range of $K_{Heat}$ | 95th | 75th | Median | 25th | 5th |
|---|---|---|---|---|---|
| 5th | 102 | 46 | 26 | 5 | 1 |
| 25th | 219 | 98 | 57 | 10 | 3 |
| Median | 275 | 124 | 71 | 13 | 3 |
| 75th | 543 | 244 | 141 | 25 | 7 |
| 95th | 663 | 298 | 172 | 31 | 8 |

**Scenario II:** d*C*/d*z*(day)=0.5·d*C*/d*z*(night)

| Range of d*C*/d*z* \ Range of $K_{Heat}$ | 95th | 75th | Median | 25th | 5th |
|---|---|---|---|---|---|
| 5th | 93 | 35 | 18 | 2 | 1 |
| 25th | 200 | 75 | 39 | 4 | 2 |
| Median | 251 | 94 | 48 | 5 | 3 |
| 75th | 496 | 187 | 96 | 11 | 5 |
| 95th | 606 | 228 | 117 | 13 | 6 |

**Scenario III:** d*C*/d*z*(day)=0.25·d*C*/d*z*(night)

| Range of d*C*/d*z* \ Range of $K_{Heat}$ | 95th | 75th | Median | 25th | 5th |
|---|---|---|---|---|---|
| 5th | 90 | 29 | 13 | 0 | 1 |
| 25th | 194 | 62 | 28 | 1 | 2 |
| Median | 244 | 77 | 35 | 1 | 2 |
| 75th | 483 | 153 | 69 | 2 | 4 |
| 95th | 589 | 187 | 84 | 3 | 5 |

(b) Phenanthrene deposition velocity ($cm \cdot s^{-1}$)

**Scenario I**

| Range of d*C*/d*z* \ Range of $K_{Heat}$ | 95th | 75th | Median | 25th | 5th |
|---|---|---|---|---|---|
| 5th | 10 | 4 | 3 | 0 | 0 |
| 25th | 21 | 9 | 5 | 1 | 0 |
| Median | 26 | 12 | 7 | 1 | 0 |
| 75th | 51 | 23 | 13 | 2 | 1 |
| 95th | 63 | 28 | 16 | 3 | 1 |

**Scenario II**

| Range of d*C*/d*z* \ Range of $K_{Heat}$ | 95th | 75th | Median | 25th | 5th |
|---|---|---|---|---|---|
| 5th | 9 | 3 | 2 | 0 | 0 |
| 25th | 19 | 7 | 4 | 0 | 0 |
| Median | 24 | 9 | 5 | 1 | 0 |
| 75th | 47 | 18 | 9 | 1 | 0 |
| 95th | 57 | 22 | 11 | 1 | 1 |

**Scenario III**

| Range of d*C*/d*z* \ Range of $K_{Heat}$ | 95th | 75th | Median | 25th | 5th |
|---|---|---|---|---|---|
| 5th | 9 | 3 | 1 | 0 | 0 |
| 25th | 18 | 6 | 3 | 0 | 0 |
| Median | 23 | 7 | 3 | 0 | 0 |
| 75th | 46 | 15 | 7 | 0 | 0 |
| 95th | 56 | 18 | 8 | 0 | 0 |

**Table S7**. Continued

(c) Anthracene flux ($pg \cdot m^{-2} s^{-1}$)

**Scenario I**

| Range of dC/dz | Range of $K_{Heat}$ | | | | |
|---|---|---|---|---|---|
| Percentile | 95th | 75th | Median | 25th | 5th |
| 5th | 3 | 1 | 1 | 0 | 0 |
| 25th | 21 | 10 | 6 | 1 | 0 |
| Median | 26 | 12 | 7 | 1 | 0 |
| 75th | 43 | 20 | 11 | 2 | 1 |
| 95th | 75 | 34 | 20 | 3 | 1 |

**Scenario II**

| Range of dC/dz | Range of $K_{Heat}$ | | | | |
|---|---|---|---|---|---|
| 95th | 75th | Median | 25th | 5th | |
| 3 | 1 | 1 | 0 | 0 | |
| 20 | 7 | 4 | 0 | 0 | |
| 24 | 9 | 5 | 1 | 0 | |
| 40 | 15 | 8 | 1 | 0 | |
| 69 | 26 | 13 | 1 | 1 | |

**Scenario III**

| Range of dC/dz | Range of $K_{Heat}$ | | | | |
|---|---|---|---|---|---|
| 95th | 75th | Median | 25th | 5th | |
| 3 | 1 | 0 | 0 | 0 | |
| 19 | 6 | 3 | 0 | 0 | |
| 23 | 7 | 3 | 0 | 0 | |
| 39 | 12 | 5 | 0 | 0 | |
| 67 | 21 | 10 | 0 | 1 | |

(d) Anthracene deposition velocity ($cm \cdot s^{-1}$)

**Scenario I**

| Range of dC/dz | Range of $K_{Heat}$ | | | | |
|---|---|---|---|---|---|
| Percentile | 95th | 75th | Median | 25th | 5th |
| 5th | 5 | 2 | 1 | 0 | 0 |
| 25th | 36 | 16 | 9 | 2 | 0 |
| Median | 43 | 19 | 11 | 2 | 1 |
| 75th | 72 | 32 | 19 | 3 | 1 |
| 95th | 125 | 56 | 32 | 6 | 2 |

**Scenario II**

| Range of dC/dz | Range of $K_{Heat}$ | | | | |
|---|---|---|---|---|---|
| 95th | 75th | Median | 25th | 5th | |
| 5 | 2 | 1 | 0 | 0 | |
| 32 | 12 | 6 | 1 | 0 | |
| 39 | 15 | 8 | 1 | 0 | |
| 66 | 25 | 13 | 1 | 1 | |
| 114 | 43 | 22 | 2 | 1 | |

**Scenario III**

| Range of dC/dz | Range of $K_{Heat}$ | | | | |
|---|---|---|---|---|---|
| 95th | 75th | Median | 25th | 5th | |
| 5 | 2 | 1 | 0 | 0 | |
| 32 | 10 | 4 | 0 | 0 | |
| 38 | 12 | 5 | 0 | 0 | |
| 64 | 20 | 9 | 0 | 1 | |
| 111 | 35 | 16 | 1 | 1 | |

**Table S7**. Continued

(e) Pyrene flux ($pg \cdot m^{-2} s^{-1}$)

**Scenario I**

| Range of dC/dz | Range of $K_{Heat}$ | | | | |
|---|---|---|---|---|---|
| Percentile | 95th | 75th | Median | 25th | 5th |
| 5th | 25 | 11 | 6 | 1 | 0 |
| 25th | 49 | 22 | 13 | 2 | 1 |
| Median | 54 | 24 | 14 | 3 | 1 |
| 75th | 112 | 50 | 29 | 5 | 1 |
| 95th | 124 | 56 | 32 | 6 | 2 |

**Scenario II**

| Range of dC/dz | Range of $K_{Heat}$ | | | | |
|---|---|---|---|---|---|
| Percentile | 95th | 75th | Median | 25th | 5th |
| 5th | 22 | 8 | 4 | 0 | 0 |
| 25th | 45 | 17 | 9 | 1 | 0 |
| Median | 49 | 19 | 10 | 1 | 0 |
| 75th | 103 | 39 | 20 | 2 | 1 |
| 95th | 114 | 43 | 22 | 2 | 1 |

**Scenario III**

| Range of dC/dz | Range of $K_{Heat}$ | | | | |
|---|---|---|---|---|---|
| Percentile | 95th | 75th | Median | 25th | 5th |
| 5th | 22 | 7 | 3 | 0 | 0 |
| 25th | 44 | 14 | 6 | 0 | 0 |
| Median | 48 | 15 | 7 | 0 | 0 |
| 75th | 100 | 32 | 14 | 0 | 1 |
| 95th | 110 | 35 | 16 | 1 | 1 |

(f) Pyrene deposition velocity ($cm \cdot s^{-1}$)

**Scenario I**

| Range of dC/dz | Range of $K_{Heat}$ | | | | |
|---|---|---|---|---|---|
| Percentile | 95th | 75th | Median | 25th | 5th |
| 5th | 22 | 10 | 6 | 1 | 0 |
| 25th | 43 | 19 | 11 | 2 | 1 |
| Median | 47 | 21 | 12 | 2 | 1 |
| 75th | 98 | 44 | 26 | 5 | 1 |
| 95th | 109 | 49 | 28 | 5 | 1 |

**Scenario II**

| Range of dC/dz | Range of $K_{Heat}$ | | | | |
|---|---|---|---|---|---|
| Percentile | 95th | 75th | Median | 25th | 5th |
| 5th | 20 | 7 | 4 | 0 | 0 |
| 25th | 39 | 15 | 8 | 1 | 0 |
| Median | 43 | 16 | 8 | 1 | 0 |
| 75th | 90 | 34 | 17 | 2 | 1 |
| 95th | 100 | 37 | 19 | 2 | 1 |

**Scenario III**

| Range of dC/dz | Range of $K_{Heat}$ | | | | |
|---|---|---|---|---|---|
| Percentile | 95th | 75th | Median | 25th | 5th |
| 5th | 19 | 6 | 3 | 0 | 0 |
| 25th | 38 | 12 | 5 | 0 | 0 |
| Median | 42 | 13 | 6 | 0 | 0 |
| 75th | 87 | 28 | 12 | 0 | 1 |
| 95th | 97 | 31 | 14 | 0 | 1 |